



Article

Up-Regulation of the Nrf2/HO-1 Antioxidant Pathway in Macrophages by an Extract from a New Halophilic Archaea Isolated in Odiel Saltworks

Javier Ávila-Román ^{1,*}, Patricia Gómez-Villegas ^{2,3,†}, Carla C. C. R. de Carvalho ^{3,4}, Javier Vígara ², Virginia Motilva ¹, Rosa León ² and Elena Talero ¹

¹ Department of Pharmacology, Faculty of Pharmacy, Universidad de Sevilla, Profesor García González Street, 41012 Seville, Spain

² Laboratory of Biochemistry, Center for Natural Resources, Health, and Environment, Universidad de Huelva, Avda. de las Fuerzas Armadas s/n, 21071 Huelva, Spain

³ iBB—Institute for Bioengineering and Biosciences, Department of Bioengineering, Instituto Superior Técnico, Universidade de Lisboa, Av. Rovisco Pais, 1049-001 Lisbon, Portugal

⁴ Associate Laboratory i4HB—Institute for Health and Bioeconomy, Instituto Superior Técnico, Universidade de Lisboa, Av. Rovisco Pais, 1049-001 Lisbon, Portugal

* Correspondence: javieravila@us.es; Tel.: +34-954559880

† These authors contributed equally to this work.

Abstract: The production of reactive oxygen species (ROS) plays an important role in the progression of many inflammatory diseases. The search for antioxidants with the ability for scavenging free radicals from the body cells that reduce oxidative damage is essential to prevent and treat these pathologies. Haloarchaea are extremely halophilic microorganisms that inhabit hypersaline environments, such as saltworks or salt lakes, where they have to tolerate high salinity, and elevated ultraviolet (UV) and infrared radiations. To cope with these extreme conditions, haloarchaea have developed singular mechanisms to maintain an osmotic balance with the medium, and are endowed with unique compounds, not found in other species, with bioactive properties that have not been fully explored. This study aims to assess the potential of haloarchaea as a new source of natural antioxidant and anti-inflammatory agents. A carotenoid-producing haloarchaea was isolated from Odiel Saltworks (OS) and identified on the basis of its 16S rRNA coding gene sequence as a new strain belonging to the genus *Haloarcula*. The *Haloarcula* sp. OS acetone extract (HAE) obtained from the biomass contained bacterioruberin and mainly C18 fatty acids, and showed potent antioxidant capacity using ABTS assay. This study further demonstrates, for the first time, that pretreatment with HAE of lipopolysaccharide (LPS)-stimulated macrophages results in a reduction in ROS production, a decrease in the pro-inflammatory cytokines TNF- α and IL-6 levels, and up-regulation of the factor Nrf2 and its target gene heme oxygenase-1 (HO-1), supporting the potential of the HAE as a therapeutic agent in the treatment of oxidative stress-related inflammatory diseases.

Keywords: bacterioruberin; carotenoids; fatty acids; haloarchaea; inflammation; macrophages; Odiel Saltworks; oxidative stress



Citation: Ávila-Román, J.; Gómez-Villegas, P.; de Carvalho, C.C.C.R.; Vígara, J.; Motilva, V.; León, R.; Talero, E. Up-Regulation of the Nrf2/HO-1 Antioxidant Pathway in Macrophages by an Extract from a New Halophilic Archaea Isolated in Odiel Saltworks. *Antioxidants* **2023**, *12*, 1080. <https://doi.org/10.3390/antiox12051080>

Academic Editors: Susana M. Cardoso, Dulcinea Ferreira Wessel and Marcelo D. Catarino

Received: 30 March 2023

Revised: 4 May 2023

Accepted: 8 May 2023

Published: 11 May 2023



Copyright: © 2023 by the authors. Licensee MDPI, Basel, Switzerland. This article is an open access article distributed under the terms and conditions of the Creative Commons Attribution (CC BY) license (<https://creativecommons.org/licenses/by/4.0/>).

1. Introduction

Many pathologies such as inflammatory bowel disease, psoriasis, and rheumatoid arthritis have an inflammatory base, triggered in part by a deficient antioxidant system that leads to ROS overproduction and chronic inflammation. Impairment of the antioxidant defense systems causes the overaccumulation of these oxidative species, which produces oxidative damage in lipids, proteins, and DNA, inducing cell death [1]. For this reason, new sources of antioxidants are desirable, not only to treat chronic diseases or promote health but also to be used as additives for food and pharmaceutical products, in order to prevent their deterioration and extend their shelf-life. Most natural antioxidants ingested by humans come from plants; however, microorganisms can also be a source of

these compounds to substitute undesirable artificial ones [2,3]. In this regard, extremely halophilic microorganisms that inhabit hypersaline environments, such as saltworks or salt lakes, are particularly interesting due to their ability to cope with extreme conditions. High salinity is the main hindrance found in these habitats, but other extreme conditions, including high ultraviolet (UV) and infrared radiations from the sun, must also be endured. Halophilic archaea are usually the main representatives of the microbiota at the highest salinity (≥ 5 M NaCl), exceeding Bacteria and Eukarya [4,5]. Haloarchaea possess specific strategies to proliferate in such harsh environments, which include the accumulation of isomolar concentrations of KCl to balance the osmotic pressure with the surrounding medium, and an adapted cellular machinery able to work at high salt concentrations [6]. In addition, Archaea count with unique cell membranes, which contain isoprenoids ether linked to *sn*-glycerol-1-phosphate, contrarily to bacterial and eukaryotic cells where the fatty acid chains are ester linked to the *sn*-glycerol-3-phosphate backbone. This lipid structure is totally different from that found in the membrane of bacteria or eukaryotes and is one of the structural characteristics that supported the definition of Archaea as an independent domain of life [7]. Previous studies have shown that several archaeal species contain fatty acids (FAs) and phospholipid FAs [8–11]; nonetheless, there is practically no information about the physiological role and the composition of haloarchaeal FAs.

Most members of the class Halobacteria are pink or red pigmented due to the presence of carotenoids and retinal proteins in their membranes [12]. Carotenoids are one of the most abundant bioactive compounds in the marine environment and are highly demanded products with many applications in cosmetics, pharmaceuticals, nutraceuticals, foods, and beverages [13]. These pigments are usually obtained from plants, algae, or yeasts, while prokaryotic microbial sources are less exploited. Interestingly, carotenoids obtained from different species of haloarchaea have been reported to exhibit health-promoting properties such as antimicrobial, antihemolytic, neuroprotective, or antiviral, among others [14–17]. The main carotenoid found in haloarchaea is bacterioruberin, a 50-carbon carotenoid with 13 conjugated double bonds and 4 terminal hydroxyl groups, which give the cells exceptional properties against oxidative stressors, acting as a radical scavenger in hypersaline environments [18]. Bacterioruberin protects the haloarchaea against UV light and could act as a membrane stabilizer, connecting the inner and outer leaflets of the membrane bilayer by the interaction of its hydroxyl groups through hydrogen bonds with the hydrophilic head groups of polar lipids [19].

In the present study, a new strain of haloarchaea belonging to the genus *Haloarcula* was isolated from Odiel Saltworks, and the antioxidant and anti-inflammatory properties of an acetone extract from this microorganism, containing carotenoids and FA, were evaluated by both in vitro and cellular assays, to explore the molecular mechanisms underlying these activities.

2. Materials and Methods

2.1. Sample Collection and Strain Isolation

Haloarchaeal strains were isolated from water samples from a crystallizer pond in Odiel Saltworks (37.255025, -6.972945), located in the Odiel River Marshlands in Huelva (SW, Spain). Water samples (20 μ L) were plated in agar plates and incubated at 37 °C for 30 days. The culture medium used for the isolation contained per liter: 10 g glucose, 156 g NaCl, 13 g $\text{MgCl}_2 \cdot 6\text{H}_2\text{O}$, 20 g $\text{MgSO}_4 \cdot 7\text{H}_2\text{O}$, 1 g $\text{CaCl}_2 \cdot 6\text{H}_2\text{O}$, 4 g KCl, 0.2 g NaHCO_3 , and 5 g yeast extract. The colony with the most intense red color was purified by five streaking rounds on fresh agar plates and preserved in 20% glycerol (*w/v*) at -80 °C for further use.

2.2. Molecular Identification

The selected microorganism was identified by 16S ribosomal RNA gene sequencing. Genome DNA was extracted by using the Gene JET Genomic Purification kit (Thermo Fisher Scientific, Waltham, MA, USA), following the manufacturer's instructions. The

full length of the 16S rRNA coding gene was amplified with specific primers for archaea 21F (5'-TTCCGGTTGATCCTGCCGGA-3') and 1492R (5'-GGTTACCTTGTTACGACTT-3'). Polymerase chain reaction (PCR) was carried out in a total volume of 25 μ L, using an Eppendorf thermo-cycler. The reaction mixture contained 1 μ L of genomic DNA, 0.2 U RED Taq[®] DNA polymerase (Sigma Aldrich, St. Louis, MO, USA), and 2.5 μ L of its specific 10 \times buffer that contained 10 pM of each primer, 0.2 mM dNTPs, and 2.5 mM MgCl₂. The thermal profile was set to 0.5 min at 96 °C, 0.5 min at 56 °C, and 1 min at 72 °C for 30 cycles, followed by 10 min of final extension. The PCR products were checked by electrophoresis, on a 1% agarose gel, and sent to Stabvida (Lisbon, Portugal) for Sanger sequencing. The 1.4 kb 16S rRNA gene sequences obtained were compared to those available at the GenBank and the European Molecular Biology Laboratory (EMBL) databases, using the Basic Local Alignment Search Tool (BLASTn) at the National Center for Biotechnology Information (NCBI) [20].

2.3. Culture Medium and Extract Preparation

The selected microorganism was grown in the liquid medium previously detailed for the strain isolation at 37 °C and 150 rpm for 10 days, and the growth was monitored according to the optical density at 580 nm. When the culture reached the stationary phase of growth, 1 L was collected by centrifugation at 19,800 \times g for 15 min at 4 °C. The cellular pellet was treated overnight with 10 mL of cold acetone (−20 °C) per gram of fresh biomass in the dark, and vortex several times until a colorless pellet was obtained. Then, the sample was centrifuged at 4 °C and 19,800 \times g for 30 min, and the supernatant, which contains carotenoids and other lipophilic compounds, was dried in a rotary vacuum evaporator and freeze dried.

2.4. Lipid Analysis

The FAs were extracted and simultaneously methylated to fatty acid methyl esters (FAMES) using the Instant FAME[™] kit from MIDI, Inc. (Newark, DE, USA), after acetone removal at 40 °C and 100 mBar on a vacuum evaporation system (RapidVap from Labconco, Kansas City, MO, USA). At least two samples of extract were used per lipid extraction. For lipid quantification, the FA C19:0 (Sigma-Aldrich, Darmstadt, Germany), was added as an internal standard prior to transesterification. The base-catalyzed kit allows the methylation of FA to FAMES and their extraction to an organic solvent for analysis.

The FAMES were analyzed by gas chromatography on a 6890N gas chromatograph, equipped with a flame ionization detector (FID) and a 7683B series injector, all from Agilent Technologies (Santa Clara, CA, USA). The gas chromatograph was equipped with a 25 m long Agilent J&W Ultra 2 capillary column and was programmed and controlled by the Sherlock software package, version 6.2 (from MIDI, Inc.). Peak identification was carried out by Sherlock Software by comparison with standards. Their identification was confirmed by injection of the same samples on an Agilent 7820A gas chromatograph equipped with a 7693A autoinjector and a 5977E quadrupole mass spectrometer (MS; Agilent Technologies, Santa Clara, CA, USA). A 25 m long Agilent J&W Ultra 2 capillary column was used, and the carrier gas was helium at 1.5 mL/min.

2.5. Carotenoid Analysis

The content of total carotenoids in the acetone extract was calculated by the absorbance of the sample at 496 nm in a cuvette with a 1 cm path length and using the specific absorption coefficient $A^{1\%} = 2540$ (100 mL g^{−1} cm^{−1}) [21]. The chromatographic analysis of the carotenoids present in the extract was performed in a Merck-Hitachi LaChrom Elite (Prague, The Czech Republic) HPLC equipped with a DAD (L-2455) detector. Separation of carotenoids was performed using an RP-18 column (5 μ m \times 25 cm \times 4.6 mm id), with an equilibration time of 20 min, and a flow rate of 1 mL min^{−1}. Solvents were (A) a mixture of acetonitrile/water (9:1 v/v) and (B) pure ethyl acetate. The gradient elution program was as follows: 0–16 min 0–60% A; 16–30 min 60% A; 30–35 min 100% A. The column temperature

was kept at 25 °C, and the injection volume was 100 µL. Chromatograms were recorded in the range of 450 nm and the EZ ChromeElite program was used for data processing. The compounds were identified on the basis of their retention time and UV–Vis spectra.

2.6. Antioxidant Capacity Assessment

The antioxidant activity of the compounds as a scavenger was performed by the ABTS colorimetric method [22]. The ABTS·+ radical was generated with 3.84 mg/mL of ABTS (Applichem, Darmstadt) and 6.6 mg/mL of potassium persulfate (Sigma-Aldrich Química, SA, Spain) dissolved in water and incubated for at least 16 h in the dark. The compounds were prepared into 96-well plates at different concentrations (0–200 µg/mL) and ABTS·+ solution, equivalent to an absorbance of 0.7 ± 0.02 , was incubated with samples for 6 min at room temperature. Then, the absorbance was measured at 734 nm by using a Synergy HT multimode microplate reader (BioTek Instruments, Winooski, VT, USA). Trolox was used as the standard antioxidant in the same concentration range. The effective concentration 50% (EC₅₀) was calculated, and results were expressed as Trolox Equivalent Antioxidant Capacity, TEAC (EC₅₀ sample/EC₅₀ Trolox).

2.7. Cell Cultures

Human acute monocytic leukemia cell line, THP-1, was purchased from the American Type Culture Collection (TIB-202, ATCC, Manassas, VA, USA) and cultured in RPMI 1640 media (GIBCO®, Life Technologies, New York, NY, USA) containing 10% heat-inactivated fetal bovine serum, 100 U/mL penicillin, and 100 mg/mL streptomycin (PAA®, Pasching, Austria), in a humidified atmosphere containing 5% CO₂ at 37 °C.

2.8. Cell Viability Assay

The in vitro cytotoxicity assessment of HAE was determined by the 3-(4,5-dimethylthiazol-2-yl)-2,5 diphenyltetrazolium bromide (MTT, Calbiochem, Darmstadt, Hesse, Germany) method [23] by using THP-1 cells transformed into macrophages. Briefly, for differentiation into macrophages, THP-1 cells were seeded into 96-well plates (100 µL/well) at a density of 10⁵ cells/mL in the presence of 8 nM phorbol 12-myristate 13-acetate (PMA, Sigma-Aldrich Química, S.A., Madrid, Spain) and, incubated in a humidified atmosphere of 5% CO₂ at 37 °C for 72 h. Afterward, the medium was removed, and cells were washed twice with ice-cold phosphate saline buffer (PBS, 4 °C). Then, the macrophages were treated with different concentrations of the acetone extract (0, 6.25, 12.5, 25, 50, and 100 µg/mL) for 24 h prepared in DMSO stock solutions at a concentration of 50 mg/mL and diluted to desired concentration directly in the culture medium. Controls were incubated in a fresh medium containing DMSO (0.2% v/v), which did not affect cell viability. Then, the cells were washed (PBS, 4 °C) prior to the addition of 100 µL of 0.25 mg/mL MTT solution into each well and were incubated for 4 h. The formazan crystals were dissolved with DMSO (200 µL) and 0.1 M glycine buffer pH 10.5 (25 µL). Finally, the absorbance was measured at 550 nm by using a Multiskan EX microplate reader (Labsystems, Thermo Scientific, Helsinki, Finland) and the 50% inhibitory concentration (IC₅₀) was calculated.

2.9. Intracellular ROS Production

The production of intracellular ROS was determined by using DCF-DA dye assay (ab113851 Abcam, Cambridge, UK) in THP-1 macrophages. Briefly, THP-1 cells were seeded into a 96-well black plate (100 µL/well) at a density of 10⁵ cells/mL with 8 nM PMA as described above. Then, the medium was removed, and cells were washed (PBS, 4 °C). Subsequently, a pretreatment with the HAE (5, 25, and 50 µg/mL), and dexamethasone (Dex) as control (1 µM) was carried out for 1 h. Then, the intracellular ROS production was induced by the addition of lipopolysaccharide from *E. coli* (LPS, 1 µg/mL) for 24 h. Control groups, unstimulated (Control) and stimulated (LPS) were incubated with a medium containing DMSO (0.2% v/v). Then, the supernatants were removed, and cells were washed (PBS, 4 °C) supplemented with 20 µM DCF-DA (100 µL/well) and incubated for

45 min, according to the manufacturer's instructions. Fluorescence was measured by using a fluorescence plate reader (Sinergy HT, Biotek[®], Bad Friedrichshall, Germany) at 485 nm for excitation and 535 nm for emission.

2.10. Determination of TNF- α and IL-6 Levels

The production of pro-inflammatory cytokines was studied in human THP-1 macrophages. Briefly, THP-1 were seeded into a 96-well plate (100 μ L/well) at a density of 10^5 cells/mL in the presence of 8 nM PMA as described previously. After differentiation, the medium was removed, and cells were washed twice (PBS, 4 °C). Subsequently, a pre-treatment with the HAE at different concentrations (5, 25, and 50 μ g/mL) and Dex (1 μ M) as positive reference compound was performed for 1 h. Then, the inflammatory response was induced by the addition of LPS (1 μ g/mL) for 24 h. Control groups were incubated with a growth medium containing DMSO (0.2% *v/v*). Afterward, the supernatants were collected and stored at -80 °C until cytokines determination by ELISA (Diacclone GEN-PROBE, Besançon, France), according to the manufacturer's protocol. The absorbance was measured with a microplate reader (Labsystems Multiskan EX, Thermo Scientific, Helsinki, Finland) at 450 nm.

2.11. Assessment of Antioxidant Proteins Expression

The expression of the antioxidant proteins Nrf2 and HO-1 was determined by Western blotting in THP-1 macrophages. Briefly, THP-1 were seeded into 6-well plates (2000 μ L/well) at a density of 4×10^5 cells/mL in the presence of 8 nM PMA as previously described. After the incubation period, the medium was removed, the cells were washed twice (PBS, 4 °C), and incubated with different concentrations of the HAE (5, 25, and 50 μ g/mL) for 1 h. The inflammatory response was induced by the addition of LPS (1 μ g/mL) for 24 h. The Control group was incubated with a growth medium containing DMSO (0.2% *v/v*). Subsequently, cell pellets were mixed with cold lysis buffer containing a cocktail of protease inhibitors (50 mM Tris-HCl pH 7.5, 8 mM MgCl₂, 5 mM ethylene glycol bis (2-aminoethyl ether)-N,N,N',N'-tetraacetic acid, 0.5 mM EDTA, 1 mM phenylmethylsulfonyl fluoride, 0.01 mg/mL leupeptin, 0.01 mg/mL pepstatin, 0.01 mg/mL aprotinin, and 250 mM NaCl (40 μ L per sample) and incubated on ice for 30 min. After that, cell homogenates were centrifugated (12,000 $\times g$, 5 min, 4 °C) to discard cell debris and DNA. The protein cytoplasmic content in the supernatants was determined using the Bradford method. Aliquots of supernatants containing equal protein (50 μ g) were separated on 10% acrylamide gel by SDS-polyacrylamide-gel electrophoresis. Then, the proteins were electrophoretically transferred onto a nitrocellulose membrane and incubated with specific primary antibodies as follows: rabbit anti-Nrf2 (1:1000) and rabbit anti-HO-1 (1:1000) (Cell Signaling, Danvers, MA, USA). Each membrane was washed three times for 10 min and incubated with the secondary horseradish peroxidase-linked anti-rabbit (Pierce Chemical, Rockford, IL, USA). To prove equal loading, the blots were analyzed for β -actin expression by using an anti- β -actin antibody (Sigma-Aldrich, St. Louis, MO, USA). Immunodetection was performed by using a chemiluminescence light-detecting kit (Super-Signal West Pico Chemiluminescent Substrate, Pierce, IL, USA). Densitometric data were analyzed following normalization to the housekeeping gene (β -actin), and the signals were quantified with Scientific Imaging Systems (Biophotonics Image J Analysis Software; National Institute of Mental Health, Bethesda, MD, USA).

2.12. Statistical Analysis

All values in the figures, tables, and text are expressed as arithmetic means \pm standard error of the mean (S.E.M.). Data were evaluated by using the GraphPad Prism Version 6.00 software (GraphPad Software, Inc., San Diego, CA, USA). The Kolmogorov–Smirnov test was used to verify the normality of the data. *p* values < 0.05 were considered statistically significant. The statistical test used for individual analyses is provided in the figure legends.

3. Results

3.1. Selection and Identification of a Carotenoid-Rich Haloarchaea

A new strain of haloarchaea was isolated from a crystallizer pond in Odiel Saltworks with 32% salinity at the moment of sampling. This microorganism was selected for its fast growth ($\mu = 1.02 \text{ days}^{-1}$), as shown in Supplementary Materials (Figure S1), and intense red color. The identification of the isolate was carried out based on the amplification and sequencing of the complete 16S rRNA encoding gene (Supplementary Materials, Figure S2). The obtained sequence was compared to those available in the NCBI database using the BLASTn tool, showing around 97.5% sequence identity with other *Haloarcu* species, such as *H. hispanica*, *H. japonica*, or *H. marismortui*. In this regard, multiple alignments were generated by Multiple Sequence Comparison by Log-Expectation (MUSCLE). Thus, it was designated as *Haloarcu* sp. OS.

A molecular phylogenetic tree was constructed by using the Molecular Evolutionary Genetics Analysis (MEGA X, Version 10, Sudhir Kumar, Pennsylvania State University, US) [24], including the new isolate *Haloarcu* sp. OS and a series of reference haloarchaeal species. The bootstrap was settled on 1000 replicates, and the thermophilic archaea *Methanococcus vulcanus* was set as an outgroup. The 16S rRNA encoding sequence of the new isolate clustered with the corresponding genes of the members of the genus *Haloarcu* (Figure 1).

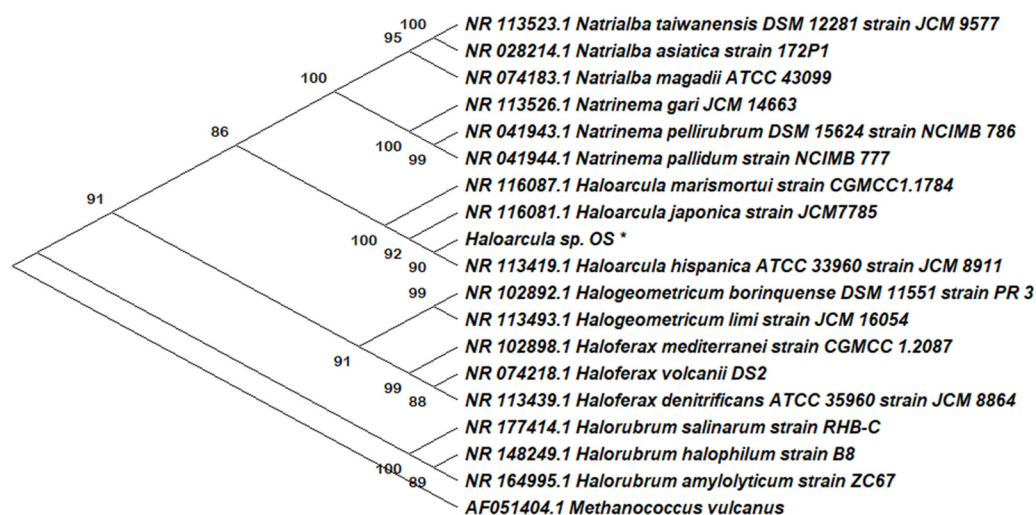


Figure 1. Molecular phylogenetic analysis by the maximum likelihood method. The tree represents a comparison within 16S rRNA coding gene sequences, including a series of reference haloarchaeal species and the new isolate, *Haloarcu* sp. OS, highlighted by an asterisk. The tree was constructed with MEGA X. The numbers at nodes indicate the bootstrap values calculated for 1000 replicates. The name and the NCBI access number are indicated for all the reference sequences. *Methanococcus vulcanus* was used as an outgroup.

3.2. Characterization of the *Haloarcu* sp. OS Acetone Extract

An acetone extract was obtained from *Haloarcu* sp. OS (HAE) with the aim of testing its potential as an antioxidant and anti-inflammatory agent. The carotenoid and FA content of this extract was analyzed by RP-HPLC-DAD and GC-MS, respectively. The elution profile of the carotenoids revealed three main peaks with identical absorption spectra with absorption maxima at 468, 496, and 532 nm and two cis absorption maxima at lower wavelengths (Figure 2), which correspond to different bacterioruberin isomers. The concentration of total bacterioruberin, the only carotenoid detected in the HAE, was 10 μg per mg of extract, calculated according to Britton (2004) [21] and using the specific absorption coefficient $A^{1\%} = 2540 (100 \text{ mL g}^{-1} \text{ cm}^{-1})$.

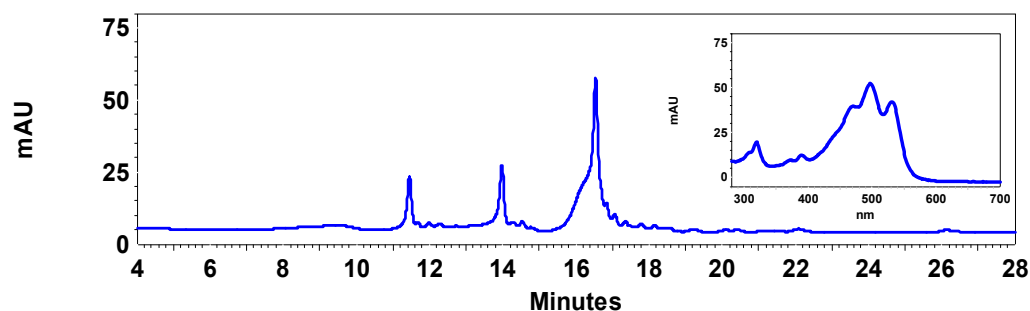


Figure 2. HPLC elution profile of the *Haloarcula* sp. OS acetone extract (HAE). The three prominent peaks observed in the chromatogram correspond to bacterioruberin isomers with the same absorption spectrum, which is shown on the insert. This UV–Vis spectrum with absorption maxima at 468, 496, and 532 nm conforms to the typical three fingers spectrum of bacterioruberin.

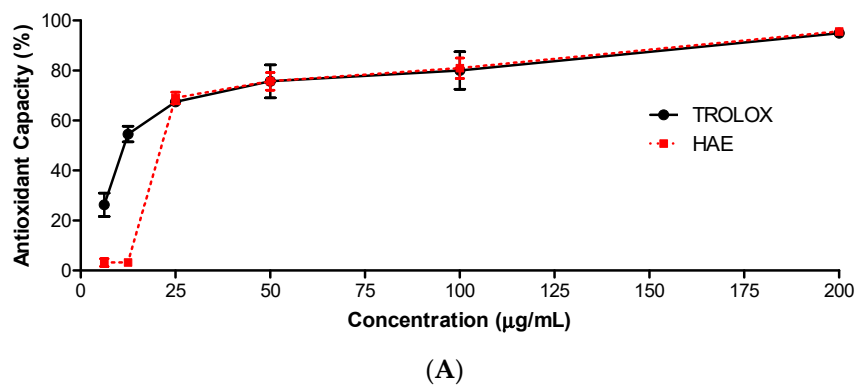
In addition to carotenoids, other lipid compounds, such as unsaturated FAs, have been shown to play an important role as antioxidants against ROS species. When the HAE was analyzed by gas chromatography-mass spectrometry, significant amounts of 16:0, 18:0, and 18:0 10-methyl FA were identified. This led to the characterization of the extract in terms of FAs. The analysis of the FAs content of the total lipids in the HAE showed that the most abundant FA was 18:0 (55.5% of total lipids), while the others accounted for ca. 0.4–14% (Table 1). The amount of FAs in the extract was $1.7 \pm 0.3 \mu\text{g FA}/\text{mg CDW}$, which corresponds to $0.8 \pm 0.06 \mu\text{g FA}/\mu\text{g extract}$.

Table 1. Fatty acid composition of the acetone extract of *Haloarcula* sp. OS (HAE) (represented in ng of fatty acids per mg of cell wet weight and as a percentage of total fatty acid content).

| FA | ng Lipids/mgCDW | % (FA/Total FAs) |
|----------------|-----------------|------------------|
| 12:0 | 36.1 | 2.1 |
| 14:0 | 8.1 | 0.5 |
| 14:0 anteiso | 8.9 | 0.5 |
| 16:0 | 101.7 | 6.0 |
| 16:0 DMA | 5.6 | 0.3 |
| 16:0 N alcohol | 62.5 | 3.7 |
| 17:0 | 7.2 | 0.4 |
| 18:0 | 948.2 | 55.5 |
| 18:0 10-methyl | 230.7 | 13.5 |
| 18:1 w9c | 95.1 | 5.6 |
| 18:2 w6c | 16.0 | 0.9 |
| 18:3 w6c | 187.4 | 11.0 |

3.3. Antioxidant Capacity of the Acetone Extract

The antioxidant capacity of the HAE was tested using the 2,2'-azino-bis (3-ethylbenzo thiazoline-6-sulfonic acid) (ABTS) method. Several dilutions of the HAE were assayed (Figure 3A) to obtain the effective concentration of 50% (EC50), which was expressed as Trolox Equivalent Antioxidant Capacity, TEAC (EC50 sample/EC50 Trolox) (Figure 3B). The reference compound Trolox showed an EC50 of $11.3 \pm 0.9 \mu\text{g}/\text{mL}$. The HAE exhibited a potent antioxidant capacity, displaying an EC50 of $20.5 \mu\text{g}/\text{mL}$. The HAE showed 1.8 equivalents of Trolox, which means that it is necessary 1.8-fold HAE than Trolox to get the same effect.



| (µg/mL) | 6.25 | 12.5 | 25 | 50 | 100 | 200 | EC50 | Eq TROLOX |
|---------|------------|------------|------------|------------|------------|------------|------------|-----------|
| TROLOX | 26.3 ± 4.6 | 54.6 ± 3.1 | 67.5 ± 1.4 | 75.7 ± 6.6 | 80.2 ± 7.5 | 94.9 ± 0.6 | 11.3 ± 0.9 | 1 |
| HAE | 3.2 ± 1.6 | 3.2 ± 0.6 | 69.0 ± 2.3 | 75.7 ± 3.5 | 80.9 ± 4.1 | 95.6 ± 0.1 | 20.5 ± 0.4 | 1.8 |

(B)

Figure 3. Scavenger antioxidant activity of the *Haloarcula* sp. OS acetone extract (HAE). (A) The antioxidant capacity of the HAE at different concentrations (0–200 µg/mL) was determined by ABTS (2,2'-azino-bis (3-ethylbenzothiazoline-6-sulfonic acid)) radical scavenging assay, using TROLOX as a reference control. (B) The half-effective concentration (EC₅₀) was calculated and the results were expressed as equivalent to Trolox (EC₅₀ sample/EC₅₀ Trolox). Results are representative of three independent experiments (n = 3).

3.4. Intracellular ROS Assessment

The levels of intracellular ROS produced in LPS-stimulated THP-1 macrophages were measured by using 2',7'-dichlorodihydrofluorescein diacetate (DCF-DA) (Figure 4). First, to rule out cytotoxic effects, the HAE was tested at different concentrations (0–100 µg/mL) by using the 3-(4,5-dimethylthiazol-2-yl)-2,5 diphenyltetrazolium bromide (MTT) method. The results showed 100% viability of the macrophages exposed to HAE at all tested concentrations for 24 h (Table 2). Based on these data, the concentrations 5, 25, and 50 µg/mL of HAE were chosen to carry out the ROS assay.

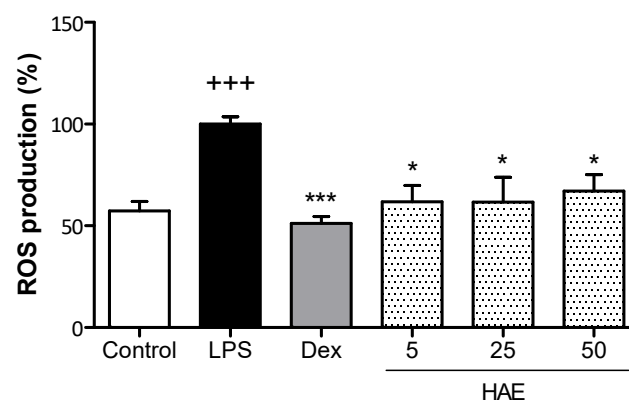


Figure 4. Effect of the *Haloarcula* sp. OS acetone extract (HAE) on the ROS production in LPS-stimulated THP-1 macrophages. THP-1 monocytes were transformed into macrophages with 8 nM PMA for 72 h. Then, cells were pretreated with the BRE (5, 25, and 50 µg/mL) for 1 h and stimulated with LPS (1 µg/mL) for 24 h. Dexamethasone (Dex, 0.39 µg/mL) was used as an internal reference control. Results are representative of four independent experiments (n = 4). Values are the means with standard errors represented by vertical bars. Mean value was significantly different compared to the Control group (+++ $p < 0.001$; Student's *t*-test). Mean value was significantly different compared to the LPS group (**+ $p < 0.001$; * $p < 0.01$; Kruskal–Wallis test).

Table 2. Viability of THP-1 human macrophages treated with different concentrations of the *Haloarcula* sp. OS acetone extract (HAE) at different concentrations. Values are the means \pm SEM (%), (N = 3).

| % Viability THP-1 Macrophages (24 h) | | | | | | |
|--------------------------------------|---------------|-----------------|-------------------|------------------|------------------|-------------------|
| ($\mu\text{g/mL}$) | 0 | 6.25 | 12.5 | 25 | 50 | 100 |
| HAE | 100 \pm 2.2 | 112.5 \pm 6.5 | 111.40 \pm 4.70 | 117.06 \pm 5.5 | 111.60 \pm 9.7 | 114.51 \pm 11.5 |

ROS production was significantly increased in the LPS group in comparison with the Control group ($p < 0.001$), which showed 57.3% of ROS basal levels. The glucocorticoid dexamethasone (Dex, 1 μM) reduced ROS production to similar levels to those of the Control group ($p < 0.001$). The treatment with the HAE caused a significant decrease in ROS production at all tested concentrations ($p < 0.05$), which achieved a reduction close to 40% in ROS levels.

3.5. Pro-Inflammatory Cytokines Levels

The *in vitro* anti-inflammatory activity of the HAE obtained from *Haloarcula* sp. OS was evaluated by measuring the production of TNF- α and IL-6 in LPS-stimulated THP-1 macrophages. Our results showed that LPS stimulation induced a marked increase in TNF- α and IL-6 production in THP-1 cells compared to unstimulated control cells ($p < 0.001$). The anti-inflammatory reference drug dexamethasone significantly reduced the levels of both cytokines ($p < 0.001$). As shown in Figure 5A, pretreatment of THP-1 cells with the HAE at the concentrations of 25 and 50 $\mu\text{g/mL}$ resulted in a significant reduction in LPS-mediated TNF- α production ($p < 0.01$ and $p < 0.001$, respectively). Furthermore, the HAE substantially reduced IL-6 levels at all tested concentrations ($p < 0.001$) (Figure 5B).

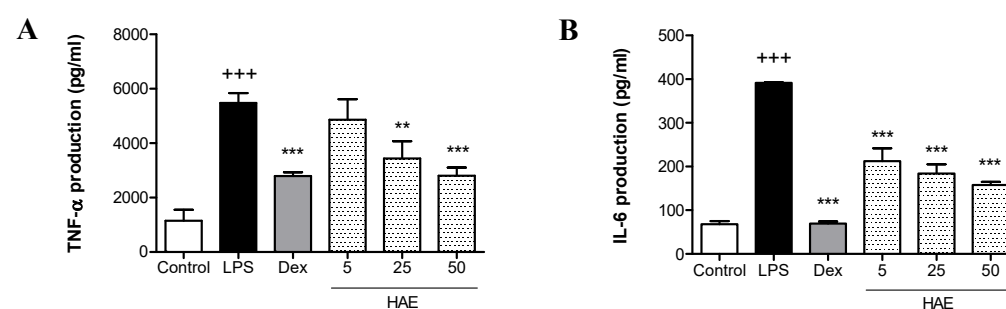


Figure 5. Effect of the *Haloarcula* sp. OS acetone extract (HAE) on the pro-inflammatory cytokines production in LPS-stimulated THP-1 macrophages. THP-1 monocytes were transformed into macrophages with 8 nM PMA for 72 h. Then, cells were pretreated with the HAE (5, 25, and 50 $\mu\text{g/mL}$) for 1 h and stimulated with LPS (1 $\mu\text{g/mL}$) for 24 h. Dexamethasone (Dex, 0.39 $\mu\text{g/mL}$) was used as an internal reference control. (A) TNF- α production. (B) IL-6 production. Results are representative of five independent experiments ($n = 5$). Values are the means with standard errors represented by vertical bars. Mean value was significantly different compared with the Control group (+++ $p < 0.001$; Student's *t*-test). Mean value was significantly different compared with the LPS group (*** $p < 0.001$, ** $p < 0.01$; ANOVA test followed by Tukey's Multiple Comparison test).

3.6. Assessment of Antioxidant Protein Expression Levels

To further explore the basis of the potential anti-inflammatory mechanisms of action of the HAE, the expression of the antioxidant proteins Nrf2 and HO-1 was evaluated by Western blotting. THP-1 macrophages were pretreated with the HAE (5, 25, and 50 $\mu\text{g/mL}$) for 1 h and then stimulated with LPS (1 $\mu\text{g/mL}$). As presented in Figure 6A, LPS stimulation did not induce significant changes in Nrf2 expression, but a slight non-significant increase in HO-1 expression was observed. However, the pretreatment with HAE resulted in a notable up-regulated expression of the Nrf2 protein at 25 and 50 $\mu\text{g/mL}$, but only the highest concentration showed a significant increase ($p < 0.05$) in LPS-stimulated macrophages

(Figure 6B). This result was correlated with a substantial increase in its target gene HO-1 at concentrations of 25 and 50 $\mu\text{g}/\text{mL}$ of the HAE ($p < 0.05$ and $p < 0.05$, respectively) (Figure 6C).

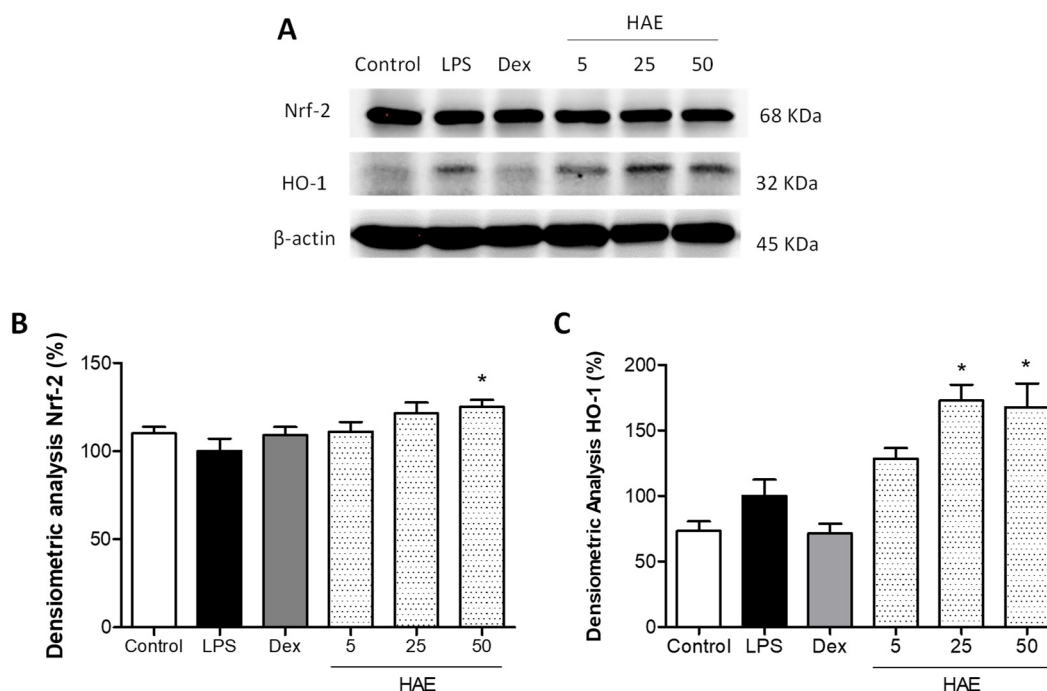


Figure 6. Effect of the *Haloarcula* sp. OS acetone extract (HAE) on the antioxidant Nrf2/HO-1 pathway in LPS-stimulated THP-1 macrophages. THP-1 monocytes were transformed into macrophages with 8 nM PMA for 72 h. Then, cells were pretreated with the HAE (5, 25, and 50 $\mu\text{g}/\text{mL}$) for 1 h and stimulated with LPS (1 $\mu\text{g}/\text{mL}$) for 24 h. Dexamethasone (Dex, 0.39 $\mu\text{g}/\text{mL}$) was used as an internal reference control. (A) Representative densitometric analysis of HO-1 and Nrf2 normalized to control (housekeeping gene, β -actin). (B) Representative Western blot analysis of Nrf2 and (C) HO-1. Results are representative of three independent experiments ($n = 3$). Values are the means with their standard errors represented by vertical bars. Mean value was compared with the Control group not showing significant differences (LPS vs. Control). Mean value was significantly different compared with the LPS group * $p < 0.05$; Kruskal–Wallis followed by Dunn’s Multiple Comparison test).

4. Discussion

The bioactive properties of haloarchaea extracts are usually linked to the antioxidant capacity of bacterioruberin. The potential of this carotenoid as a radical scavenger has been demonstrated in vitro by several chemical assays (DPPH, ABTS, FRAP, etc.) in different genera of halophilic archaea [15,25,26]. However, the lack of studies on human cell lines makes it difficult to define the pharmacological importance of haloarchaea-derived carotenoids and to extrapolate these results to the development of drugs or health promotion approaches. In this regard, the results obtained in our study have demonstrated, for the first time, the anti-inflammatory properties of HAE in LPS-induced THP-1 macrophages through up-regulation of the Nrf2/HO-1 antioxidant pathway.

Although bacterioruberin is the main carotenoid found in haloarchaea, [27–29], the extracts obtained from these microorganisms contain other types of molecules that could potentially have bioactive properties. In this study, we demonstrate that along with bacterioruberin, several membrane FAs are also present in the HAE, being C18:0 the most abundant. It is not always accepted that some archaeal species produce significant amounts of FA, although it has been shown that phospholipid FAs may represent 11–32% of total phospholipids-derived side chains in Archaea and 89% in *M. fervidus* [9]. In fact, Archaea have interesting lipids, containing ether linkages, which provide these cells high resilience

in environments with high salt concentrations [30,31]. Diether phospholipids in Archaea, which are mirror images of the diester glycerophospholipids found in all other organisms, may also protect them against stereospecific phospholipases excreted by other organisms in competitive environments [30]. In the family *Halobacteriaceae*, the core lipid that is the basis for the most polar lipid structures is 2,3-di-*O*-phytanyl-*sn*-glycerol, with monomethylated phosphatidylglycerophosphate (PGP-Me) being the main phospholipid [32]. The closest species to *Haloarcula* sp. OS, *H. japonica*, *H. marismortui*, and *H. hispanica*, also contain *sn*-2,3-di-*O*-phytanyl-glycerol exclusively as a core lipid [33,34]. Significant amounts of phospholipid FAs have been previously found in other archaea, including *Halobacterium halobium*, *Methanobacterium thermoautotrophicum*, *Methanococcus jannaschii*, and *Methanopyrus kandleri* [9]. The FA composition of the phospholipids affects the fluidity/rigidity of the cellular membrane in bacteria [35]. Archaeal cells have isoprenoid chains, which are functional over a wide range of temperatures and conditions and, thus, they do not require a regulatory mechanism to adapt lipids during, e.g., environmental temperature changes [36]. However, bacterioruberin is known to increase membrane rigidity in haloarchaea [37].

Accumulating evidence has revealed that oxidative stress and inflammation play a key role in the development and progression of many pathologies, including atopic dermatitis, psoriasis, inflammatory bowel disease, cardiovascular disease, and cancer, among others. It has been shown that in an inflammatory process, immune cells release large amounts of ROS, which induce damage to macromolecules such as DNA, lipids, and proteins, as well as lead to the production of pro-inflammatory mediators [38]. For this reason, the discovery of new agents that attenuate the inflammatory process and oxidative stress can prevent the development of these chronic pathological conditions. Firstly, our results evidenced the antioxidant capacity of the HAE extracted from the new *Haloarcula* sp. OS strain by using ABTS assays. Therefore, the antioxidant activity of the HAE in LPS-stimulated THP-1 macrophages was further evaluated as an *in vitro* model of oxidative stress. HAE significantly reduced intracellular ROS production induced by LPS, thus protecting cells from oxidative stress. These results are consistent with a variety of studies reporting the antioxidant activity of carotenoids [39,40], and also of plant and microbial extracts [41–44].

Overproduction of ROS results in the release of high levels of pro-inflammatory cytokines such as TNF- α and IL-6. These cytokines can activate immune cells to generate more inflammatory mediators and amplify the immune inflammatory response, leading to tissue damage [45]. In the present study, HAE exerted marked anti-inflammatory activity through the reduction in TNF- α and IL-6 production. Consistent with these findings, there is only one study that evaluates the anti-inflammatory activity of nanoparticles containing a bacterioruberin extract plus dexamethasone. These authors reported that these nanoparticles reduced ROS and TNF- α levels to a higher extent than dexamethasone nanoparticles in a gut inflammation model consisting of Caco-2 cells and LPS-stimulated THP-1 cells [46].

Nrf2 is a redox-sensitive transcription factor that under oxidative stress translocates to the nucleus and activates the expression of antioxidant genes such as HO-1. Previous studies have shown that the increase in Nrf2-mediated HO-1 has anti-inflammatory effects through the inhibition of many pro-inflammatory mediators, including TNF- α and IL-6 [47]. It is worth highlighting that the results of our study reported that dexamethasone, a strong and widely used glucocorticoid, decreased ROS production and levels of pro-inflammatory cytokines TNF- α and IL-6 in LPS-stimulated THP-1 macrophages, but its mechanism of action does not appear to be linked to the Nrf/HO-1 signaling pathway. Therefore, HAE involves an antioxidant and anti-inflammatory alternative to classical glucocorticoids such as dexamethasone. Furthermore, LPS-stimulated THP-1 macrophages showed an increase in HO-1 protein expression but not Nrf2 protein expression, which may be explained by an activation of Nrf2 basal cellular levels in response to increased LPS-induced ROS levels. Our results demonstrate that HAE significantly increased the Nrf2 and its main target gene HO-1 protein expression at 50 $\mu\text{g}/\text{mL}$. Additionally, although HAE at 25 $\mu\text{g}/\text{mL}$ did not show increased Nrf2 expression, a significant up-regulation of HO-1 expression level was

observed, suggesting that HAE may also induce the activation of the Nrf2 basal cellular levels. These findings suggest that up-regulation of the Nrf2/HO-1 signaling pathway may prevent LPS-induced increase in the pro-inflammatory cytokines TNF- α and IL-6. Consistent with these results, a previous study by our group demonstrated that carotenoid fucoxanthin increased the expression of Nrf-2/HO-1 proteins in a UVB-induced erythema model in mice, protecting skin against UV exposure [48].

Additionally, it is well known that the bioaccessibility and bioavailability of carotenoids depend on the proportion of these molecules solubilized in micelles that are formed with other lipophilic compounds, such as FAs, cholesterol and phospholipids [49]. In fact, FAs-containing lipids, especially those containing unsaturated bonds, can contribute to scavenger activity and could have a synergic antioxidant effect with carotenoids, improving their bioavailability and harnessing their transport across cell membranes due to their amphipathic nature [49]. In accordance with these observations, we hypothesized that FAs present in the HAE may contribute to the antioxidant activity of the bacterioruberin.

It is well established that diets rich in polyunsaturated FAs and pigments, as well as the use of these compounds in supplements, have significant health benefits [35]. The HAE contained mainly C18 FAs, including the branched 18:0 10-methyl, and the polyunsaturated 18:2 w6c and 18:3 w6c. Branched-chain FAs, which also include *iso* and *anteiso* FAs, have been found to have a beneficial anti-inflammatory role by increasing the expression of IL-10 [50], as well as 18:2 w6c and 18:3 w6c have been associated to a lower risk of rheumatoid arthritis [51] and anti-inflammatory and antithrombotic properties [52,53].

Based on the results of the present paper, the authors are aware of the limitations of this study but also its potential. In this regard, we have only performed in vitro experimental work with an acetone extract enriched in the carotenoid bacterioruberin and FAs. Therefore, further studies focused on optimizing culture conditions would be of interest to obtain extracts or batches with a similar composition in FAs and bacterioruberin, as well as higher amounts of bacterioruberin *per se*, since this promising carotenoid is poorly investigated. On the other hand, the potential of HAE as an antioxidant/anti-inflammatory agent has been evidenced in the present work, but additional in vivo bioaccessibility and bioavailability studies are necessary to demonstrate its therapeutic potential and explore further mechanistic studies. Numerous studies on the lipid composition, including FAs and carotenoids, of, e.g., microalgae have been published but studies on the composition of Archaea are still scarce [54,55]. Our study suggests that the latter are necessary for future biotechnological applications of Archaea.

5. Conclusions

In summary, the results show that the new strain *Haloarcula* sp. OS isolated from Odiel Salworks produces the carotenoid bacterioruberin and significant amounts of FAs. The findings show that the HAE exhibits high antioxidant capacity by the ABTS method. In addition, this study demonstrates, for the first time, that the HAE reduces LPS-induced oxidative stress and acute inflammation in THP-1 macrophages by attenuating both ROS levels and the production of the pro-inflammatory cytokines TNF- α and IL-6. The mechanisms underlying these protective effects are related, at least in part, to the activation of the Nrf-2/HO-1 signaling pathway. Furthermore, the HAE involves an alternative mechanism of action to classical glucocorticoids as dexamethasone. These contributions support the potential use of HAE as a therapeutic agent in the treatment of oxidative stress-related inflammatory diseases.

Supplementary Materials: The following supporting information can be downloaded at: <https://www.mdpi.com/article/10.3390/antiox12051080/s1>, Figure S1: Growth curve of the isolated haloarchaea *Haloarcula* sp. OS (HAE); Figure S2: Full length of the 16S rRNA encoding gene from *Haloarcula* sp. OS, amplified with the archaeal-specific primers 21F (5'-TTCCGGTTGATCCTGCCGGA-3') and 1492R (5'-GGTTACCTTGTTACGACTT-3').

Author Contributions: Conceptualization, E.T., R.L. and V.M.; formal analysis J.Á.-R., P.G.-V., C.C.C.R.d.C., V.M. and E.T.; funding acquisition, V.M., P.G.-V., C.C.C.R.d.C., R.L., J.V. and E.T.; investigation, J.Á.-R., P.G.-V., E.T. and V.M.; methodology, J.Á.-R., P.G.-V. and C.C.C.R.d.C.; writing—original draft, J.Á.-R., P.G.-V. and E.T.; writing—review and editing, J.Á.-R., P.G.-V., C.C.C.R.d.C., J.V., V.M., R.L. and E.T. All authors have read and agreed to the published version of the manuscript.

Funding: This research was funded by the Operative FEDER Program-Andalucía 2014–2020 (US-1380844 and UHU-1257518), Spanish Agencia Estatal de Investigación (PID2019-110438RB-C22-AEI/FEDER), the Andalusian government (I+D+i-JA-PAIDI-Retos projects 2020-PY20) and the “VII Plan Propio de Investigación y Transferencia” of The University of Seville. The work was partially funded by national funds from Fundação para a Ciência e a Tecnologia (FCT, Portugal) in the scope of the projects UIDB/04565/2020 and UIDP/04565/2020 of the Research Unit iBB—Institute for Bioengineering and Biosciences, and of the project LA/P/0140/2020 of the i4HB—Associate Laboratory Institute for Health and Bioeconomy. P.G.-V acknowledges financial support from the “Margarita Salas” grant for the training of young doctors, University of Huelva.

Institutional Review Board Statement: Not applicable.

Informed Consent Statement: Not applicable.

Data Availability Statement: Not applicable.

Acknowledgments: We thank “Centro de Investigación, Tecnología e Innovación (CITIUS)” at The University of Seville for providing technical assistance.

Conflicts of Interest: The authors declare no conflict of interest.

References

1. Mittal, M.; Siddiqui, M.R.; Tran, K.; Reddy, S.P.; Malik, A.B. Reactive oxygen species in inflammation and tissue injury. *Antioxid. Redox Signal.* **2014**, *20*, 1126–1167. [[CrossRef](#)] [[PubMed](#)]
2. Chandra, P.; Sharma, R.K.; Arora, D.S. Antioxidant compounds from microbial sources: A review. *Food Res. Int.* **2020**, *129*, 108849. [[CrossRef](#)] [[PubMed](#)]
3. Rani, A.; Saini, K.C.; Bast, F.; Mehariya, S.; Bhatia, S.K.; Lavecchia, R.; Zuurro, A. Microorganisms: A potential source of bioactive molecules for antioxidant applications. *Molecules* **2021**, *26*, 1142. [[CrossRef](#)]
4. Oren, A. The microbiology of red brines. In *Advances in Applied Microbiology*; Elsevier Inc.: Amsterdam, The Netherlands, 2020; Volume 113, pp. 57–110. ISBN 9780128207093.
5. Gómez-Villegas, P.; Vigar, J.; León, R. Characterization of the microbial population inhabiting a solar saltern pond of the odiel Marshlands (SW Spain). *Mar. Drugs* **2018**, *16*, 332. [[CrossRef](#)]
6. Oren, A. Life at high salt concentrations, intracellular KCl concentrations, and acidic proteomes. *Front. Microbiol.* **2013**, *4*, 315. [[CrossRef](#)]
7. Lombard, J.; López-García, P.; Moreira, D. An ACP-independent fatty acid synthesis pathway in archaea: Implications for the origin of phospholipids. *Mol. Biol. Evol.* **2012**, *29*, 3261–3265. [[CrossRef](#)]
8. Carballeira, N.M.; Reyes, M.; Sostre, A.; Huang, H.; Verhagen, M.F.J.M.; Adams, M.W.W. Unusual fatty acid compositions of the hyperthermophilic archaeon *Pyrococcus furiosus* and the bacterium *Thermotoga maritima*. *J. Bacteriol.* **1997**, *179*, 2766–2768. [[CrossRef](#)]
9. Gattinger, A.; Schloter, M.; Munch, J.C. Phospholipid etherlipid and phospholipid fatty acid fingerprints in selected euryarchaeotal monocultures for taxonomic profiling. *FEMS Microbiol. Lett.* **2002**, *213*, 133–139. [[CrossRef](#)]
10. Gattinger, A.; Günthner, A.; Schloter, M.; Munch, J.C. Characterisation of Archaea in soils by polar lipid analysis. *Acta Biotechnol.* **2003**, *23*, 21–28. [[CrossRef](#)]
11. Hamerly, T.; Triplet, B.; Wurch, L.; Hettich, R.L.; Podar, M.; Bothner, B.; Copié, V. Characterization of Fatty Acids in Crenarchaeota by GC-MS and NMR. *Archaea* **2015**, *2015*, 472726. [[CrossRef](#)]
12. de Carvalho, C.C.R.; Caramujo, M.J. Carotenoids in aquatic ecosystems and aquaculture: A colorful business with implications for human health. *Front. Mar. Sci.* **2017**, *4*, 93. [[CrossRef](#)]
13. Kirti, K.; Amita, S.; Priti, S.; Mukesh Kumar, A.; Jyoti, S. Colorful World of Microbes: Carotenoids and Their Applications. *Adv. Biol.* **2014**, *2014*, 837891. [[CrossRef](#)]
14. Hou, J.; Cui, H.L. In Vitro Antioxidant, Antihemolytic, and Anticancer Activity of the Carotenoids from Halophilic Archaea. *Curr. Microbiol.* **2018**, *75*, 266–271. [[CrossRef](#)] [[PubMed](#)]
15. Gómez-Villegas, P.; Vigar, J.; Vila, M.; Varela, J.; Barreira, L.; León, R. Antioxidant, antimicrobial, and bioactive potential of two new haloarchaeal strains isolated from odiel salterns (Southwest Spain). *Biology* **2020**, *9*, 298. [[CrossRef](#)]

16. Lizama, C.; Romero-Parra, J.; Andrade, D.; Riveros, F.; Bórquez, J.; Ahmed, S.; Venegas-Salas, L.; Cabalín, C.; Simirgiotis, M.J. Analysis of carotenoids in haloarchaea species from atacama saline lakes by high resolution uhplc-q-orbitrap-mass spectrometry: Antioxidant potential and biological effect on cell viability. *Antioxidants* **2021**, *10*, 1230. [[CrossRef](#)]
17. Hegazy, G.E.; Abu-Serie, M.M.; Abo-Elela, G.M.; Ghozlan, H.; Sabry, S.A.; Soliman, N.A.; Abdel-Fattah, Y.R. In Vitro dual (anticancer and antiviral) activity of the carotenoids produced by haloalkaliphilic archaeon *Natrialba* sp. M6. *Sci. Rep.* **2020**, *10*, 5986. [[CrossRef](#)]
18. Saito, T.; Miyabe, Y.; Ide, H.; Yamamoto, O. Hydroxyl radical scavenging ability of bacterioruberin. *Radiat. Phys. Chem.* **1997**, *50*, 267–269. [[CrossRef](#)]
19. Kellermann, M.Y.; Yoshinaga, M.Y.; Valentine, R.C.; Wörmer, L.; Valentine, D.L. Important roles for membrane lipids in haloarchaeal bioenergetics. *Biochim. Biophys. Acta Biomembr.* **2016**, *1858*, 2940–2956. [[CrossRef](#)]
20. Altschul, S.F.; Gish, W.; Miller, W.; Myers, E.W.; Lipman, D.J. Basic local alignment search tool. *J. Mol. Biol.* **1990**, *215*, 403–410. [[CrossRef](#)]
21. Britton, G.; Liaaen-Jensen, S.; Pfander, H. *Carotenoids*, 1st ed.; Britton, G., Liaaen-Jensen, S., Pfander, H., Eds.; Birkhäuser Basel: Basel, Switzerland, 2004; ISBN 978-3-7643-6180-8.
22. Re, R.; Pellegrini, N.; Proteggente, A.; Pannala, A.; Yang, M.; Rice-Evans, C. Antioxidant activity applying an improved ABTS radical cation decolorization assay. *Free Radic. Biol. Med.* **1999**, *26*, 1231–1237. [[CrossRef](#)]
23. Twentyman, P.R.; Luscombe, M. A study of some variables in a tetrazolium dye (MTT) based assay for cell growth and chemosensitivity. *Br. J. Cancer* **1987**, *56*, 279–285. [[CrossRef](#)] [[PubMed](#)]
24. Kumar, S.; Stecher, G.; Li, M.; Niyaz, C.; Tamura, K. MEGA X: Molecular evolutionary genetics analysis across computing platforms. *Mol. Biol. Evol.* **2018**, *35*, 1547–1549. [[CrossRef](#)] [[PubMed](#)]
25. Sahli, K.; Gomri, M.A.; Esclapez, J.; Gómez-Villegas, P.; Bonete, M.-J.; León, R.; Kharroub, K. Characterization and biological activities of carotenoids produced by three haloarchaeal strains isolated from Algerian salt lakes. *Arch. Microbiol.* **2022**, *204*, 6. [[CrossRef](#)] [[PubMed](#)]
26. Alvares, J.J.; Furtado, I.J. Characterization of multicomponent antioxidants from *Haloferax alexandrinus* GUSF-1 (KF796625). *Biotech* **2021**, *11*, 58. [[CrossRef](#)]
27. Squillaci, G.; Parrella, R.; Carbone, V.; Minasi, P.; La Cara, F.; Morana, A. Carotenoids from the extreme halophilic archaeon *Haloterrigena turkmenica*: Identification and antioxidant activity. *Extremophiles* **2017**, *21*, 933–945. [[CrossRef](#)]
28. Naziri, D.; Hamidi, M.; Hassanzadeh, S.; Tarhriz, V.; Zanjani, B.M.; Nazemyieh, H.; Hejazi, M.A.; Hejazi, M.S. Analysis of carotenoid production by *Halorubrum* sp. TBZ126; an extremely halophilic archeon from Urmia Lake. *Adv. Pharm. Bull.* **2014**, *4*, 61–67. [[CrossRef](#)] [[PubMed](#)]
29. Yatsunami, R.; Ando, A.; Yang, Y.; Takaichi, S.; Kohno, M.; Matsumura, Y.; Ikeda, H.; Fukui, T.; Nakasone, K.; Fujita, N.; et al. Identification of carotenoids from the extremely halophilic archaeon *Haloarcula japonica*. *Front. Microbiol.* **2014**, *5*, 100. [[CrossRef](#)] [[PubMed](#)]
30. Corcelli, A.; Lobasso, S. 25 Characterization of Lipids of Halophilic Archaea. In *Methods in Microbiology*; Academic Press: Cambridge, MA, USA, 2006; Volume 35, pp. 585–613. ISBN 9780125215374.
31. Corcelli, A.; Chong, P.L.G.; Koga, Y. Lipid biology of archaea. *Archaea* **2012**, *2012*, 710836. [[CrossRef](#)]
32. Kate, M. Membrane lipids of archaea. In *New Comprehensive Biochemistry*; Elsevier: Amsterdam, The Netherlands, 1993; Volume 26, pp. 261–295. [[CrossRef](#)]
33. Morita, M.; Yamauchi, N.; Eguchi, T.; Kakinuma, K. Structural Diversity of the Membrane Core Lipids of Extreme Halophiles. *Biosci. Biotechnol. Biochem.* **1998**, *62*, 596–598. [[CrossRef](#)]
34. de Souza, L.M.; Müller-Santos, M.; Iacomini, M.; Gorin, P.A.J.; Sasaki, G.L. Positive and negative tandem mass spectrometric fingerprints of lipids from the halophilic Archaea *Haloarcula marismortui*. *J. Lipid Res.* **2009**, *50*, 1363–1373. [[CrossRef](#)]
35. de Carvalho, C.C.C.R.; Caramujo, M.J. The various roles of fatty acids. *Molecules* **2018**, *23*, 2583. [[CrossRef](#)] [[PubMed](#)]
36. Koga, Y. Thermal adaptation of the archaeal and bacterial lipid membranes. *Archaea* **2012**, *2012*, 789652. [[CrossRef](#)] [[PubMed](#)]
37. Lazrak, T.; Wolff, G.; Albrecht, A.M.; Nakatani, Y.; Ourisson, G.; Kates, M. Bacterioruberins reinforce reconstituted *Halobacterium* lipid membranes. *Biochim. Biophys. Acta Biomembr.* **1988**, *939*, 160–162. [[CrossRef](#)]
38. Leyane, T.S.; Jere, S.W.; Houreld, N.N. Oxidative Stress in Ageing and Chronic Degenerative Pathologies: Molecular Mechanisms Involved in Counteracting Oxidative Stress and Chronic Inflammation. *Int. J. Mol. Sci.* **2022**, *23*, 7273. [[CrossRef](#)]
39. Avila-Roman, J.; Garda-Gil, S.; Rodriguez-Luna, A.; Motilva, V.; Talero, E. Anti-inflammatory and anticancer effects of microalgal carotenoids. *Mar. Drugs* **2021**, *19*, 531. [[CrossRef](#)]
40. Bohn, T.; Bonet, M.L.; Borel, P.; Keijer, J.; Landrier, J.F.; Milisav, I.; Ribot, J.; Riso, P.; Winklhofer-Roob, B.; Sharoni, Y.; et al. Mechanistic aspects of carotenoid health benefits—Where are we now? *Nutr. Res. Rev.* **2021**, *34*, 276–302. [[CrossRef](#)]
41. Moopantakath, J.; Imchen, M.; Anju, V.T.; Martínez-espinoza, R.M.; Kumavath, R. Bioactive molecules from haloarchaea: Scope and prospects for industrial and therapeutic applications. *Front. Microbiol.* **2023**, *14*, 1113540. [[CrossRef](#)]
42. Assunção, M.F.G.; Amaral, R.; Martins, C.B.; Ferreira, J.D.; Ressurreição, S.; Santos, S.D.; Varejão, J.M.T.B.; Santos, L.M.A. Screening microalgae as potential sources of antioxidants. *J. Appl. Phycol.* **2017**, *29*, 865–877. [[CrossRef](#)]
43. Rodrigues, M.J.; Neves, V.; Martins, A.; Rauter, A.P.; Neng, N.R.; Nogueira, J.M.F.; Varela, J.; Barreira, L.; Custódio, L. In vitro antioxidant and anti-inflammatory properties of *Limonium algarvense* flowers' infusions and decoctions: A comparison with green tea (*Camellia sinensis*). *Food Chem.* **2016**, *200*, 322–329. [[CrossRef](#)]

44. Saeed, N.; Khan, M.R.; Shabbir, M. Antioxidant activity, total phenolic and total flavonoid contents of whole plant extracts *Torilis leptophylla* L. *BMC Complement. Altern. Med.* **2012**, *12*, 221. [[CrossRef](#)]
45. Checa, J.; Aran, J.M. Reactive oxygen species: Drivers of physiological and pathological processes. *J. Inflamm. Res.* **2020**, *13*, 1057–1073. [[CrossRef](#)] [[PubMed](#)]
46. Higa, L.H.; Schilrreff, P.; Briski, A.M.; Jerez, H.E.; de Farias, M.A.; Villares Portugal, R.; Romero, E.L.; Morilla, M.J. Bacterioruberin from *Haloarchaea* plus dexamethasone in ultra-small macrophage-targeted nanoparticles as potential intestinal repairing agent. *Colloids Surf. B Biointerfaces* **2020**, *191*, 110961. [[CrossRef](#)] [[PubMed](#)]
47. Saha, S.; Buttari, B.; Panieri, E.; Profumo, E.; Saso, L. An Overview of Nrf2 Signaling Pathway and Its Role in Inflammation. *Molecules* **2020**, *25*, 5474. [[CrossRef](#)] [[PubMed](#)]
48. Rodríguez-Luna, A.; Ávila-Román, J.; González-Rodríguez, M.L.; Cózar, M.J.; Rabasco, A.M.; Motilva, V.; Talero, E. Fucoxanthin-containing cream prevents epidermal hyperplasia and UVB-induced skin erythema in mice. *Mar. Drugs* **2018**, *16*, 378. [[CrossRef](#)]
49. Molteni, C.; La Motta, C.; Valoppi, F. Improving the Bioaccessibility and Bioavailability of Carotenoids by Means of Nanostructured Delivery Systems: A Comprehensive Review. *Antioxidants* **2022**, *11*, 1931. [[CrossRef](#)]
50. Ran-Ressler, R.R.; Khailova, L.; Arganbright, K.M.; Adkins-Rieck, C.K.; Jouni, Z.E.; Koren, O.; Ley, R.E.; Brenna, J.T.; Dvorak, B. Branched chain fatty acids reduce the incidence of necrotizing enterocolitis and alter gastrointestinal microbial ecology in a neonatal rat model. *PLoS ONE* **2011**, *6*, e29032. [[CrossRef](#)]
51. De Pablo, P.; Romaguera, D.; Fisk, H.L.; Calder, P.C.; Quirke, A.M.; Cartwright, A.J.; Panico, S.; Mattiello, A.; Gavrilu, D.; Navarro, C.; et al. High erythrocyte levels of the n-6 polyunsaturated fatty acid linoleic acid are associated with lower risk of subsequent rheumatoid arthritis in a southern European nested case-control study. *Ann. Rheum. Dis.* **2018**, *77*, 981–987. [[CrossRef](#)]
52. Rengachar, P.; Bhatt, A.N.; Polavarapu, S.; Veeramani, S.; Krishnan, A.; Sadananda, M.; Das, U.N. Gamma-Linolenic Acid (GLA) Protects against Ionizing Radiation-Induced Damage: An In Vitro and In Vivo Study. *Biomolecules* **2022**, *12*, 797. [[CrossRef](#)]
53. Shiels, K.; Tsoupras, A.; Lordan, R.; Zabetakis, I.; Murray, P.; Kumar Saha, S. Anti-inflammatory and antithrombotic properties of polar lipid extracts, rich in unsaturated fatty acids, from the Irish marine cyanobacterium *Spirulina subsalsa*. *J. Funct. Foods* **2022**, *94*, 105124. [[CrossRef](#)]
54. Sun, X.M.; Ren, L.J.; Zhao, Q.Y.; Ji, X.J.; Huang, H. Microalgae for the production of lipid and carotenoids: A review with focus on stress regulation and adaptation. *Biotechnol. Biofuels* **2018**, *11*, 272. [[CrossRef](#)]
55. Fernandes, A.S.; Nascimento, T.C.; Pinheiro, P.N.; Vendruscolo, R.G.; Wagner, R.; de Rosso, V.V.; Jacob-Lopes, E.; Zepka, L.Q. Bioaccessibility of microalgae-based carotenoids and their association with the lipid matrix. *Food Res. Int.* **2021**, *148*, 110596. [[CrossRef](#)] [[PubMed](#)]

Disclaimer/Publisher’s Note: The statements, opinions and data contained in all publications are solely those of the individual author(s) and contributor(s) and not of MDPI and/or the editor(s). MDPI and/or the editor(s) disclaim responsibility for any injury to people or property resulting from any ideas, methods, instructions or products referred to in the content.